Mathematical Biosciences and Engineering

http://www.aimspress.com/journal/MBE

MBE, 17(4): 2853–2861.
DOI: 10.3934/mbe.2020159
Received: 04 March 2020
Accepted: 16 March 2020
Published: 26 March 2020

Research article

The within-host viral kinetics of SARS-CoV-2

Chentong Li[1], Jinhu Xu[2], Jiawei Liu[3] and Yicang Zhou[1,*]

[1] School of Mathematics and Statistics, Xi'an Jiaotong University, Xi'an, 710049, China
[2] School of Sciences, Xi'an University of Technology, Xi'an, 710048, China
[3] Department of Ecology and Evolution, University of Chicago, Chicago, IL 60637, USA

* **Correspondence:** Email: zhouyc@xjtu.edu.cn; Tel: +862982668741; Fax: +862982668741.

Abstract: In this work, we use a within-host viral dynamic model to describe the SARS-CoV-2 kinetics in the host. Chest radiograph score data are used to estimate the parameters of that model. Our result shows that the basic reproductive number of SARS-CoV-2 in host growth is around 3.79. Using the same method we also estimate the basic reproductive number of MERS virus is 8.16 which is higher than SARS-CoV-2. The PRCC method is used to analyze the sensitivities of model parameters. Moreover, the drug effects on virus growth and immunity effect of patients are also implemented to analyze the model.

Keywords: SARS-CoV-2; MERS; differential equation model; basic reproductive number

1. Introduction

At the end of 2019, a new type of coronavirus, severe acute respiratory syndrome coronavirus 2 (SARS-CoV-2), began to threaten the people in China, especially in Hubei province. As of March 14, 2020, 81,026 individuals have been confirmed to be infected by this virus in China, including 3194 deaths. To mitigate the spread of the virus, the Chinese Government has progressively implemented metropolitan-wide quarantine in Wuhan and several nearby cities from Jan 23–24, 2020 [1]. The virus has also spread to several other countries, such as the Republic of Korea, Japan, Italy, and the USA. Around the world, many new deaths are reported every day. The government of many countries, such as Italy and Korea, introduce measures to control traffic flow, block cities, and establish temporary hospitals to slow down the transmission of the virus and treat the patients. Meanwhile, scientists all around the world are trying them best to find methods to analyze the structure of the virus protein [2], the viral phylodynamics [3], and develop the vaccine of that virus [4] to protect us.

Computed tomography of chest (Chest CT) and chest radiograph are used to assess the severity of lung involvement in coronavirus disease 2019 (COVID-19) [5], which is the name of that new

coronavirus caused disease [6]. Before Feb 13, the new cases in China were confirmed by nucleic acid testing. After that day, the diagnostic criterion has been improved, composed of not only the nucleic acid testing but also the CT test. The destructed pulmonary parenchyma and the resulting inflammation can be reflected from the chest radiograph [7]. Chest radiograph score method is a useful way to quantify the destruction of pulmonary parenchyma and in this study, our data set is based on this.

Several works are [1, 8] nowcasting and forecasting the number of confirmed cases of COVID-19. Meanwhile, some works [9, 10] overview the characteristics, exposure history, and illness timelines of confirmed cases. All of these work focus on population dynamics of COVID-19, while, the works about the viral dynamics in host are rare. In this work, we use the within-host viral dynamic model [11, 12] to describe the SARS-CoV-2 kinetics in host and the parameters of that model are estimated via the chest radiograph score. Moreover, using the CT score data of Middle East respiratory syndrome (MERS) that shown in Oh et al. [7], the paramters of MERS coronavirus are also estimated as a comparision group. All of the results are shown in the third section.

2. Method

We use the following ordinary differential equation model to simulate the coronavirus within-lung growth:

$$\begin{cases} \dfrac{dE_p(t)}{dt} = d_E\Big(E_p(0) - E_p(t)\Big) - \beta E_p(t)v(t), \\ \dfrac{dE_p^*(t)}{dt} = \beta E_p(t)v(t) - d_{E^*}E_p^*(t), \\ \dfrac{dv(t)}{dt} = \pi_v E_p^*(t) - d_v v(t), \end{cases} \tag{2.1}$$

where $E_p(t)$, $E_p^*(t)$ and $v(t)$ are the number of uninfected pulmonary epithelial cells, infected pulmonary epithelial cells and the virus. β is the infection rate of virus, π_v is the virus production rate, $E_p(0)$ is the number of uninfected epithelial cells without virus, and the term $d_E E_p(0)$ assumes a constant regeneration of uninfected epithelial cells. d_E, d_{E^*} and d_v are the death rate of uninfected pulmonary epithelial cells, infected pulmonary epithelial cells and the virus, respectively. The death rate of $E_p(t)$ is the natural clearance rate of pulmonary epithelial cells, while, d_{E^*} and d_v are the combination of the natural clearance rate and elimination by the immunity system. This model was also used to describe the within-lung infection process of flu virus [12, 13].

By the definition of generation matrix of basic reproductive number R_0 [14], the R_0 of model (2.1) can be written as,

$$R_0 = \frac{\beta \pi_v E_p(0)}{d_{E^*} d_v}. \tag{2.2}$$

This number is an important value to measure whether the epidemic or species could die out or not [15]. In this study, the sensitivity analysis result of R_0 is shown in the next section.

In this study, the chest radiograph score data from serve patients (with high chest radiograph scores) are collected from the work of Pan et al. [5] and Oh et al. [7]. Our estimation is based on these two data sets. We consider the chest radiograph score as a way to reflect the infected pulmonary epithelial cells [5, 7], which is also the target attacked by the immune cell [16]. Thus by the Poisson distribution,

the likelihood that used to extimate parameters can be written as,

$$L = \sum_i \Big(D_i \log \Big(E_p^*(t_i) \Big) - E_p^*(t_i) - \log \Gamma(D_i + 1) \Big), \tag{2.3}$$

where D_i is the smoothed chest radiograph score of the serve patient at time t_i, $E_p^*(t_i)$ is the solution of $E_p^*(t)$ at time t_i, and $\log \Gamma(x)$ is log-gamma function, respectively. The prior distributions of the parameters of model (2.1) are based on the previous work [13,17]. Based on that likelihood, the Monte Carlo Markov Chain (MCMC) method, which is a commonly used method in paramter estimation, is used to estimate all of the parameters of model (2.1).

3. Results

Figure 1 shows the fitted result of our model. In that figure, the chain of solutions is calculated by the chain of parameters that generated in the MCMC method, and 95% Highest Posterior Density interval is computed by the `hdi()` function from R package 'HDInterval'. Table 1 summarizes the estimation results of the parameters and R_0 of our model (2.1). We estimate that the death rate of these two virus are 5.36 (COVID-19) and 4.64 (MERS) per day, which is larger than the clearance rate of the virus on the outside surface [18]. This result shows the immune system can clear the virus directly. The estimation result also shows that the R_0 of SARS-CoV-2 in serve patients is around the mean value 3.79 which is lower than that of MERS virus (8.16). These results illustrate that the immune system can not clear the virus effectively at the beginning time of symptom onset. By these estimated parameters of COVID-19, the solutions of model (2.1) are illustrated in Figure 2.

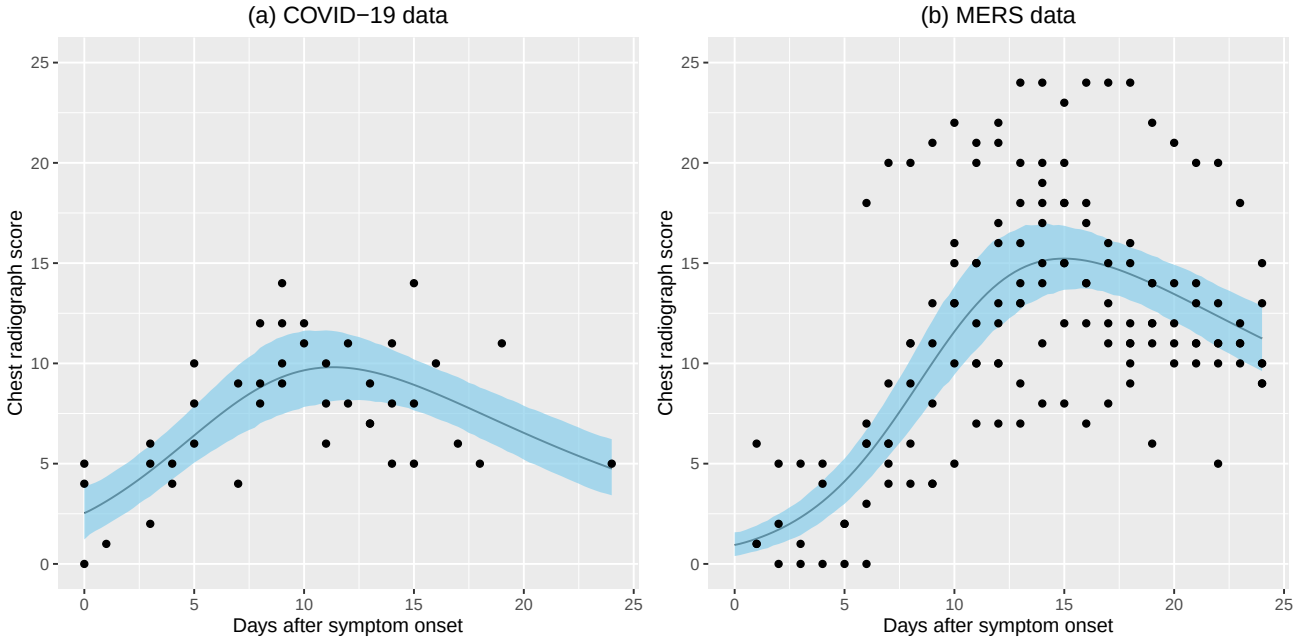

Figure 1. The chest radiograph score data and fitted result of (a) COVID-19, and (b) MERS. The dark line is the mean value of fitted result, while, the 95% Highest Posterior Density interval is shown in blue. The black points are the chest radiograph score data.

Table 1. Model parameters.

Parameter	Description (units)	Mean value of COVID-19 (std)	Mean value of MERS (std)	Source
$E_p(t_0)$	The value of uninfected epithelial cells when symptom onset(score)	$25 - E_{p^*}(t_0)$	$25 - E_{p^*}(t_0)$	[5, 7]
$E_{p^*}(t_0)$	The value of infected epithelial cells when symptom onset (score)	2.59 (0.61)	0.89 (0.28)	MCMC
$v(t_0)$	The initial value of virus when symptom onset (score)	0.061 (0.0503)	0.0075 (0.0099)	MCMC
π_v	Virus production rate per infected epithelial cells (day^{-1})	0.24 (0.22)	0.15 (0.16)	MCMC
β	Infection rate of epithelial cells by virus ($\text{day}^{-1}\text{score}^{-1}$)	0.55 (0.55)	1.28 (1.37)	MCMC
d_E	Death rate of epithelial cells (day^{-1})	10^{-3}	10^{-3}	[13]
d_{E^*}	Death rate of infected epithelial cells (day^{-1})	0.11 (0.01)	0.056 (0.0053)	MCMC
d_v	Death rate of virus (day^{-1})	5.36 (6.42)	4.64 (0.89)	MCMC
R_0	basic reproductive number	3.79 (0.54)	8.16 (1.13)	MCMC

[a] The t_0 here is the symptom onset time.

Table 2. Sensitivity of R_0 with respect to $E_p(0)$, β, π_v, d_{E^*}, and d_v.

Parameter	Range	PRCC	95% CI
$E_p(0)$	$(20, 30)$	0.9132	$(0.913, 0.9134)$
β	$(0.44, 0.66)$	0.9132	$(0.913, 0.9134)$
π_v	$(0.192, 0.288)$	0.9132	$(0.9129, 0.9134)$
d_{E^*}	$(0.088, 0.132)$	-0.9132	$(-0.9134, -0.9129)$
d_v	$(4.288, 6.432)$	-0.9132	$(-0.9134, -0.9129)$

The partial rank correlation coefficient (PRCC) method [19] is used to do the sensitivity analysis of R_0. The result (Table 2) shows that the parameters $E_p(0)$, β, π_v, d_{E^*}, and d_v have almost the same level of influence on R_0. Parameters d_{E^*}, and d_v have negative correlations with R_0, while $E_p(0)$, β, π_v have positive correlations. The positive correlation of $E_p(0)$ with R_0 may give a explanation on why the babys, who have small amount of pulmonary epithelial cells, are not likely to get infected and have lower mortality (see [10], Table 1).

Drug therapy is also a topic discussed widely on viral dynamics [11]. For the coronavirus there are some drugs that may have a positive influence on decreasing the virus load [20]. The simulation about the drug effect are shown in Figure 3. In this simulation, we take the value of parameters that shown in Table 1 as the baseline parameters, and assume the drug can drop the infection rate β to 0.1β. These results show that the earlier to give an effective drug to a serve patient, the better to relieve symptoms.

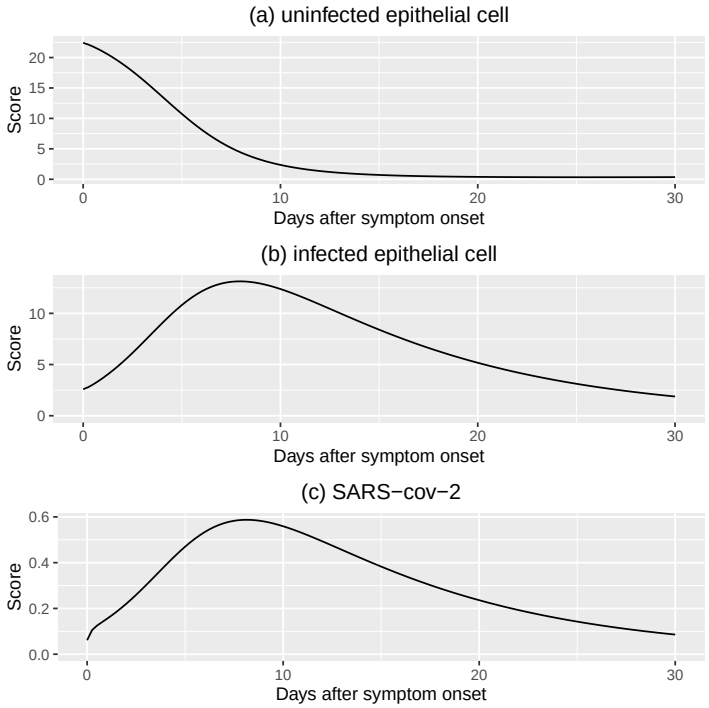

Figure 2. The solutions of model (2.1) with the parameters of COVID-19 that shown in Table 1.

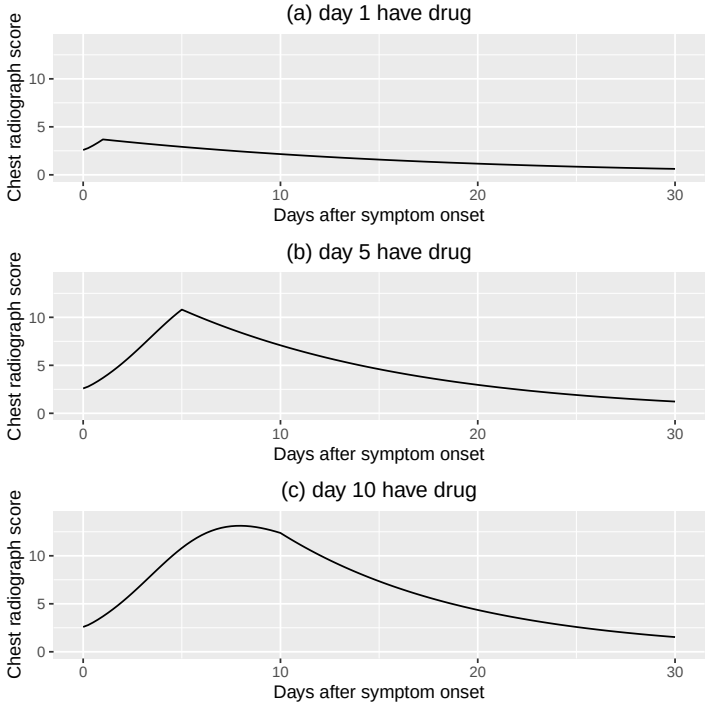

Figure 3. The simulated result of chest radiograph score of patients with COVID-19 and the beginning time of having drug is (a) the first day, (b) the fifth day, and (c) the tenth day after symptom onset. In this simulation, the drug effect is assumed to decrease the infection rate β to 0.1β.

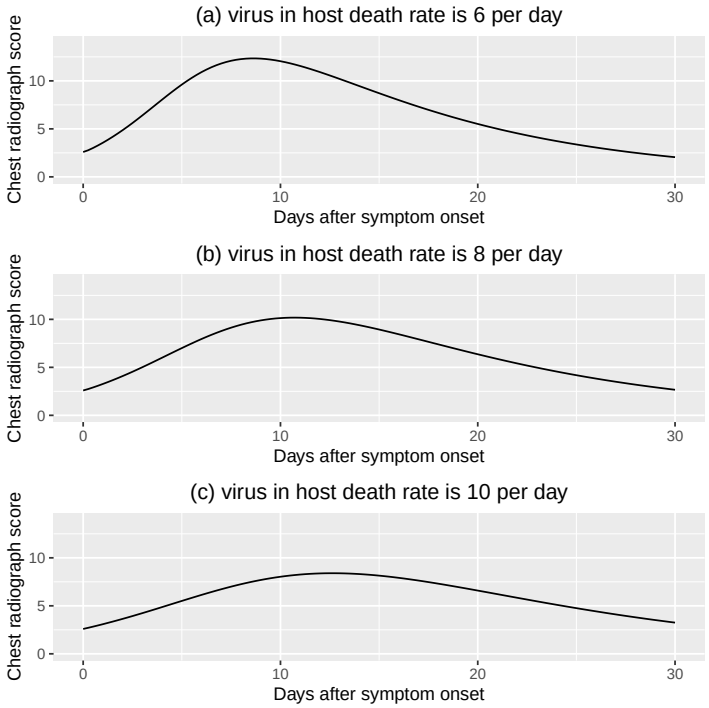

Figure 4. The simulated result of chest radiograph score of patients with COVID-19 and death rate of virus is (a) 6 per day, (b) 8 per day and (c) 10 per day.

When the symptom is onset, the immunity system already have worked to clear the virus [16]. But, the patients are at different ages and their immune capacities are different. In Figure 4, the simulation results show that the virus with a higher death rate can relieve the symptom of patients, Patients have a stronger immune system, can clear the virus better, and have milder symptoms. This result may explain why the young are easy to recover from this disease (see [10]).

In Figure 5, the simulation results show that with a higher initial value of the virus, the symptom of patients is more severe. This means the individuals who have more possible to exposure to the virus (such as the doctors fighting with COVID-19 and the workers treating the medical waste of COVID-19 patients) should much more take care of themselves.

4. Discussion

Based on the chest radiograph data, we estimate the parameters and basic reproductive number of the model (2.1). The R_0 of SARS-CoV-2 in host growth is 3.79, which is higher than hepatitis C virus (mean value as 2.26, [21]), but lower than the flu virus (mean value as 23, [17]). Comparing the estimated parameters of SARS-CoV-2 with MERS coronavirus, the MERS have a higher virulence to infect the pulmonary epithelial cells (larger R_0) and with a small value of infected cell when symptom onset. These may esplain why the MERS have a higher mortality and smaller incubation period [7, 9]. By the PRCC method, the sensitivity analysis is also done on the R_0, and the positive correlation of $E_p(0)$ with R_0 may give a possible reason why the baby patients are less likely to die of this virus.

In this manuscript, three simulations about our model are done to study how the different factors can influence the symptoms of patients. These results illustrate that (1) early medication is effective

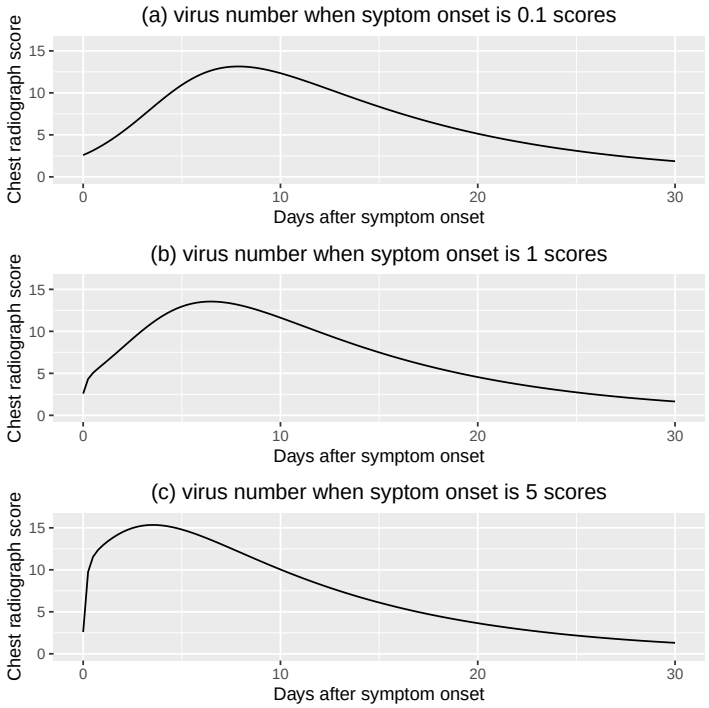

Figure 5. The simulated result of chest radiograph score of patients with COVID-19 and the number of virus when symptom onset is (a) 0.1 scores, (b) 1 scores and (c) 5 scores.

for treatment, (2) patients with strong immunity have fewer symptoms, and (3) people who are often exposed to the virus are more likely to become severe.

The methods we used in this study are following the previous works by Miao et al. [12, 17]. This is the first time for this methodology to be used in the COVID-19 and our work shows some new results of the within-host properties of this virus. All of the source codes are available at the GitHub (`https://github.com/ChentongLi/SARS-CoV-2_viral_kinetic`). Anyone could use these codes to estimate and forecast the chest radiograph score of the patients.

The major limitation of this study is that the chest radiograph score is not the real data of the infected pulmonary epithelial cells but just an approximation. Moreover, we assume that the immunne effect on viruses and infected epithelial cells are constant values. This is because the data of antibody and effective CD8 cells of that virus are rarely known. If we could get more accurate data, the results will be much better.

We believe this study could give some help to the diagnosis and treatment of the COVID-19. For other disease that infect the lung, this method we believe also could be used to do analysis.

Acknowledgments

This work is supported by National Natural Science Foundation of China (11701445), Natural Science Basic Research Plan in Shaanxi Province of China (2018JQ1057), and Young Talent Fund of University Association for Science and Technology in Shaanxi, China (20180504).

Conflict of interest

The authors declare there is no conflict of interest.

References

1. J. T. Wu, K. Leung, G. M. Leung, Nowcasting and forecasting the potential domestic and international spread of the 2019-ncov outbreak originating in wuhan, china: a modelling study, *Lancet*, 2020.
2. S. F. Ahmed, A. A. Quadeer, M. R. McKay, Preliminary identification of potential vaccine targets for the covid-19 coronavirus (sars-cov-2) based on sars-cov immunological studies, *Viruses*, **12** (2020), 254.
3. H. W. Elsland, Y. Wang, Report 5: Phylogenetic analysis of sars-cov-2.
4. W. Shang, Y. Yang, Y. Rao, X. Rao, The outbreak of sars-cov-2 pneumonia calls for viral vaccines, *npj Vaccines*, **5** (2020), 1–3.
5. F. Pan, T. Ye, P. Sun, S. Gui, B. Liang, L. Li, et al., Time course of lung changes on chest ct during recovery from 2019 novel coronavirus (covid-19) pneumonia, *Radiology*, (2020), 200370.
6. WHO, Coronavirus disease (covid-19) outbreak, 2020. Available from: `https://www.who.int/emergencies/diseases/novel-coronavirus-2019`.
7. M. Oh, W. B. Park, P. G. Choe, S. Choi, J. Kim, J. Chae, et al., Viral load kinetics of mers coronavirus infection, *N. Engl. J. Med.*, **375** (2016), 1303–1305.
8. T. Liu, J. Hu, M. Kang, L. Lin, H. Zhong, J. Xiao, et al., Transmission dynamics of 2019 novel coronavirus (2019-ncov), 2020.
9. Q. Li, X. Guan, P. Wu, X. Wang, L. Zhou, Y. Tong, et al., Early transmission dynamics in wuhan, china, of novel coronavirus–infected pneumonia, *N. Engl. J. Med.*, 2020.
10. The Novel Coronavirus Pneumonia Emergency Response Epidemiology Team, The epidemiological characteristics of an outbreak of 2019 novel coronavirus diseases (covid-19) in china, *Chin. J. Epidemiol.*, **41** (2020), 145–151.
11. S. Bonhoeffer, R. M. May, G. M. Shaw, M. A. Nowak, Virus dynamics and drug therapy, *Proc. Natl. Acad. Sci. USA*, **94** (1997), 6971–6976.
12. H. Miao, X. Xia, A. S. Perelson, H. Wu, On identifiability of nonlinear ode models and applications in viral dynamics, *SIAM Rev.*, **53** (2011), 3–39.
13. H. Y. Lee, D. J. Topham, S. Y. Park, J. Hollenbaugh, J. Treanor, T. R Mosmann, et al., Simulation and prediction of the adaptive immune response to influenza a virus infection, *J. Virol.*, **83** (2009), 7151–7165.
14. O. Dieckmann, J. P. Heesterbeek, Mathematical epidemiology of infectious diseases, 2000.
15. W. Wang, X. Zhao, Threshold dynamics for compartmental epidemic models in periodic environments, *J. Dyn. Differ. Equ.*, **20** (2008), 699–717.
16. NCBI, The innate and adaptive immune systems, 2010. Available from: `https://www.ncbi.nlm.nih.gov/books/NBK279396/#_i2255_theadaptiveimmunesys_`.

17. H. Miao, J. A. Hollenbaugh, M. S. Zand, J. Holden-Wiltse, T. R. Mosmann, A. S. Perelson, et al., Quantifying the early immune response and adaptive immune response kinetics in mice infected with influenza a virus, *J. Virol.*, **84** (2010), 6687–6698.
18. G. Kampf, D. Todt, S. Pfaender, E. Steinmann, Persistence of coronaviruses on inanimate surfaces and its inactivation with biocidal agents, *J. Hosp. Infect.*, 2020.
19. S. Marino, I. B. Hogue, C. J. Ray, D. E. Kirschner, A methodology for performing global uncertainty and sensitivity analysis in systems biology, *J. Theor. Biol.*, **254** (2008), 178–196.
20. H. Lu, Drug treatment options for the 2019-new coronavirus (2019-ncov), *BioSci. Trends*, **14** (2020), 69–71.
21. S. DebRoy, B. M. Bolker, M. Martcheva, Bistability and long-term cure in a within-host model of hepatitis c, *J. Biol. Syst.*, **19** (2011), 533–550.

AIMS Press